Computationally-Efficient Structural Health Monitoring using Graph Signal Processing

Muhammad Asaad Cheema, *Member, IEEE,* Muhammad Zohaib Sarwar,
Vinay Chakravarthi Gogineni, *Senior Member, IEEE,* Daniel Cantero,
and Pierluigi Salvo Rossi, *Senior Member, IEEE*

***Abstract*—Structural health monitoring (SHM) of bridges is crucial for ensuring safety and long-term durability, however, standard damage-detection algorithms are computationally intensive. This paper proposes a computationally-efficient algorithm based on graph signal processing (GSP) to leverage the underlying network structure in the data. Under the assumption that damages impact both spatial and temporal structures of the sensors data, the algorithm combines spatial and temporal information from accelerometers by computing the smoothness of graph signals expanded along time. The Kullback-Leibler (KL) divergence is used as dissimilarity metric to distinguish between healthy condition and presence of a damage, while Tukey's method for outliers removal and sequential detection via exponential Weighted moving average (EWMA) are then employed for performance improvement. The proposed GSP-based SHM system is appealing in terms of simplicity and low-complexity, and is also suitable for real-time monitoring. The effectiveness in terms of detection performance is validated both on synthetically-generated data and real-world measurements.**

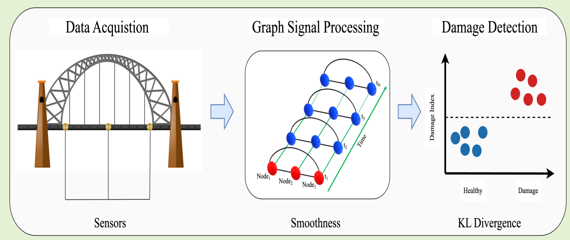

***Index Terms*—Structural health monitoring (SHM), graph signal processing (GSP), joint graph Laplacian, KL divergence, KW51 bridge, finite element model.**

I. Introduction

DIGITALIZATION is pervading several areas ranging from entertainment activities to industrial applications. Real-time monitoring and anomaly detection are among the relevant topics being enhanced by the development and integration of digital solutions into safety-critical systems, given the capability of processing data collected by sensors deployed in environments of interest.

Structural Health Monitoring (SHM) is an interdisciplinary field playing a crucial role in civil engineering relying on the integration of signal processing, data mining, and sensor technology. SHM aims at safety by enabling cost-effective predictive maintenance of civil infrastructures such as buildings and bridges [1]. For efficient monitoring, sensors are strategically placed at various locations on these structures, leading to the generation of spatio-temporal data usually arranged into multivariate time series.

Graph signal processing (GSP) is an effective approach for analyzing data originating from irregular and complex structures. GSP extends classic signal processing tools (e.g. Fourier analysis and filtering) with application to graph-based structures and has established the groundwork for developing novel graph-based learning algorithms [2]. These developments have attracted considerable attention from researchers across various fields encompassing applications from detecting faulty sensors [3] to advancements in coal mining [4].

SHM and GSP appears to be a good match given the relevance of the spatial information related to the topology of the physical structure to be monitored and the potential improvements in terms of performance and computational complexity. In this work, we investigate the feasibility of a GSP-based SHM approach for damage detection of bridges. Aging bridge infrastructures worldwide pose growing challenges due to increased mobility, traffic volume, and climate change, which accelerate their deterioration [5], [6]. Current procedures for bridge maintenance primarily depend on manual and visual inspections, which are costly, time-consuming and largely subjective. Hence, the demand for more efficient and objective SHM approaches, is pressing [7].

This work was partially supported by the Research Council of Norway under the project ML4ITS within the IKTPLUSS framework.

M. A. Cheema and P. Salvo Rossi are with the Department of Electronic Systems, Faculty of Information Technology and Electrical Engineering, Norwegian University of Science and Technology (e-mail: asaad.cheema@ntnu.no, salvorossi@ieee.org).

M. Z. Sarwar and D. Cantero are with the Department of Structural Engineering, Faculty of Engineering, Norwegian University of Science and Technology (e-mail: muhammad.z.sarwar, daniel.cantero@ntnu.no).

V. C. Gogineni is with the Applied AI and Data Science Unit, The Maersk Mc-Kinney Moller Institute, University of Southern Denmark, Denmark (e-mail: vigo@mmmi.sdu.dk).

A. Related Work

Amongst SHM techniques, those based on vibrations have gained substantial attention due to their capability to record the comprehensive behaviour of the structure and detect damages without any prior information related to the the damaged area [8]. Vibration-based SHM techniques for damage detection can essentially be divided into two groups: (i) model-based methods and (ii) data-driven methods.

Methods from the former group rely on numerical models alongside experimental data to assess the structural integrity and mostly rely on measuring and processing strain. Despite their popularity and precision, these methods present high computational complexity, making them unsuitable for large-scale SHM applications [9]. Recently, edge-computing has been considered as an opportunity to reduce the amount of data sharing in SHM systems [10].

Data-driven approaches mainly use data mining and advanced signal processing techniques to extract valuable information directly from the sensor data collected from the target bridge. Although the training phase might be computationally expensive, data-driven methods are more suitable for real-time damage detection in large structures, given less-intensive computational requirements during operation [11]. Among data-driven approaches, cable losses in a cable-stayed bridge were assessed via identification of rotation influence lines by instrumenting only two locations at the bridge bearings [12]. Similarly, accelerometers were used to identify structural rotation and related influence lines to detect damages due to the loss of bending stiffness in the bridge deck [13], [14]. Also, low- and band-pass filters were shown to detect damage-sensitive structural features from acceleration measurements [15], [16]. First-order eigen-perturbation techniques for SHM have been discussed in [17], [18] for the identification of the structural modal parameters and damage assessment.

It is worth noticing that despite the performance in terms of damage evaluation, the practical application of most approaches to SHM is still challenging due to the need of data obtained from continuous bridge monitoring [19]. However, in real-world scenarios, continuous monitoring is extremely challenging (and sometimes not practical) due to various constraints (e.g. limited power, limited bandwidth, difficulties with batteries replacement) particularly when reliant on wireless sensor networks [20] [21]. Thus, event-triggered sensing systems have emerged, designed to focus on significant portions of data, reduce power consumption and promote enduring operation of sensor nodes [22].

Furthermore, while most data-driven research on damage assessment in bridges has focused on the use of ambient vibration data or static effects, recent studies recognize vehicle-induced or forced responses as useful for performing damage assessment [23]. These recent monitoring techniques and related data interpretations have been explored with application to both highway and railway bridges [24]. Artificial neural networks have been proposed for classifying bridge health and damage states using deck acceleration and bridge weigh-in-motion data [25], [26]. Long-short-term-memory neural networks and other deep neural network have been explored focusing on reducing the number of false alarms due to sensor failures [27]. Other SHM methods include time series analysis for global monitoring of railway bridges [28] and the use of autoregressive models to extract damage-sensitive features from traffic-induced vibration responses [29]. Finally, optical fibre networks have shown to provide relevant benefits, especially as an alternative when conventional sensors cannot capture peak strains [30], while some preliminary results on the development of data-driven SHM monitoring systems based on non-contact sensing techniques (e.g. based on image processing) are found in [31].

In summary, most existing works and methodologies have certain limitations, such as requiring data from the continuous monitoring of the bridge or performing computationally-expensive training of deep neural networks. To overcome these limitations, this study aims to develop a methodology based on GSP that can extract damage-sensitive features from data generated by trains crossing by utilizing limited amount of data, eliminate the need for continuous monitoring.

B. Contribution and Paper Organization

Motivated by the previous discussion, this paper presents an effective algorithm for detecting structural damages on bridges. The algorithm leverages GSP techniques to extract information from data acquired by sensors mounted on the bridge using forced response. The algorithm incorporates the knowledge of sensor placement on the bridge to extract the underlying graph structure and relies on the concepts of *smoothness* and Kullback-Leibler (KL) divergence. The main contribution of the paper is the following.

- The proposed method adopts an event-based approach focusing on forced vibrations where data is collected in relation to particular events (such as a vehicle or train crossing the bridge), thus, unlike continuous monitoring systems, being energy efficient.
- The proposed method relies on tools from GSP to integrate the topology of the sensor network together with the measured data from the sensors.
- The proposed algorithm is computationally efficient and does not require learning any parameter.
- Perforamnce has been assessed on both synthetic data from numerical simulations and realistic data from real-world measurements.

The remainder of this paper is organized as follows. Sec. II presents the fundamentals of GSP, while the GSP-based SHM approach is described in detail in Sec. III. Sec. IV provides a description of the datasets considered for the validation of the proposed approach (one dataset is synthetically generated from numerical simulations and one dataset is collected from real-world measurements). The corresponding achieved performance are presented and discussed in Sec. V, which includes also a comparison with one of the common traditional approaches in structural engineering. Finally, Sec. VI summarizes the paper and adds some final remarks.

Notations - Lower-case (resp. upper-case) bold letters denote column vectors (resp. matrices), with a_i (resp. $A_{i,j}$) representing the ith entry (resp. (i,j)th entry) of $\boldsymbol{a}$ (resp.

$\boldsymbol{A}$); $\mathrm{diag}(\boldsymbol{a})$ denotes a diagonal matrix with $\boldsymbol{a}$ on the main diagonal; $\mathbf{I}$ is the identity matrix; upper-case calligraphic letters denote finite sets, with $|\mathcal{A}|$ being the cardinality of $\mathcal{A}$; $\mathbb{R}$ denotes the set of real numbers; $(\cdot)^{\mathrm{T}}$, $\mathrm{tr}(\cdot)$ and $\|\cdot\|$ denote transpose, trace and Euclidean norm operators, respectively; $\times$ is the Cartesian product.

II. Preliminaries of Graph Signal Processing

We describe the main concepts of graph signal processing necessary for the development of the proposed SHM approach. More specifically, we focus on discussing the graph Laplacian matrix and the graph Fourier transform (GFT) in Secs. II-A and the normalized smoothness II-B.

A sensor network is usefully represented via an undirected graph $\mathcal{G}(\mathcal{V},\mathcal{E},\boldsymbol{A})$, where $\mathcal{V}$ represents the set of $N=|\mathcal{V}|$ nodes (i.e., sensors), $\mathcal{E}$ represents the set of edges (i.e., the connection among the nodes), and $\boldsymbol{A}\in\mathbb{R}^{N\times N}$ is the adjacency matrix describing the connectivity of the graph[1], which is defined as

$$A_{i,j}=\begin{cases}1 & \text{node } i \text{ and node } j \text{ are connected}\\ 0 & \text{else}\end{cases} .$$

A graph signal is defined by a vector $\boldsymbol{x}\in\mathbb{R}^N$ where the ith element x_i collects the value from the ith node in the corresponding graph $\mathcal{G}$.

A. Graph Laplacian and Graph Fourier Transform

For a given graph $\mathcal{G}(\mathcal{V},\mathcal{E},\boldsymbol{A})$, we define the *graph Laplacian matrix* as

$$\boldsymbol{L}=\boldsymbol{D}-\boldsymbol{A}\,, \tag{1}$$

where the degree matrix $\boldsymbol{D}$ is a diagonal matrix whose entries on the main diagonal are $D_{i,i}=\sum_{j=1}^{N}A_{i,j}$. The graph Laplacian matrix is one of the most relevant operators in graph signal processing as its eigendecomposition defines the GFT [32]. More specifically, $\boldsymbol{L}=\boldsymbol{Q}\boldsymbol{\Lambda}\boldsymbol{Q}^{\mathrm{T}}$ defines the orthogonal matrix of eigenvectors $\boldsymbol{Q}\in\mathbb{R}^{N\times N}$, namely the graph Fourier basis, and the diagonal matrix $\boldsymbol{\Lambda}=\mathrm{diag}\left(\lambda_1,\dots,\lambda_N\right)$ with $\lambda_1\leq\dots\leq\lambda_N$ being the corresponding eigenvalues, namely the spatial frequencies.

The GFT of the graph signal $\boldsymbol{x}$ defined on $\mathcal{G}$ is given by $\boldsymbol{x}_{\mathcal{F}}=\boldsymbol{Q}^{\mathrm{T}}\boldsymbol{x}=\left[\boldsymbol{q}_1^{\mathrm{T}}\boldsymbol{x},\dots,\boldsymbol{q}_N^{\mathrm{T}}\boldsymbol{x}\right]^{\mathrm{T}}$. It is worth noticing that the ith element of the GFT corresponds to the projection of the graph signal onto the ith eigenvector.

B. Normalized Smoothness

The level of variation in a graph signal (i.e. how similar are the values on neighboring nodes) is a relevant information, which might be related to anomalies [33]. It may be inferred via the *normalized smoothness*, formally defined as

$$s_{\mathcal{G}}(\boldsymbol{x})=\frac{\boldsymbol{x}^{\mathrm{T}}\boldsymbol{L}\boldsymbol{x}}{\|\boldsymbol{x}\|^2}\,. \tag{2}$$

[1]More general representations for the graph connectivity are possible.

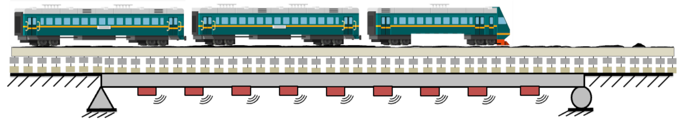

Fig. 1: Schematic example of a bridge equipped with sensors collecting information when a train is traversing it.

More specifically, exploiting the egiendecomposition of the graph Laplacian matrix, Eq. (2) can be expressed as

$$s_{\mathcal{G}}(\boldsymbol{x})=\sum_{i=1}^{N}\frac{\lambda_i}{\|\boldsymbol{x}\|^2}\left\|\boldsymbol{q}_i^{\mathrm{T}}\boldsymbol{x}\right\|^2\,,$$

which shows how the smoothness is a linear combination of the energy content of frequency components $\boldsymbol{q}_i^{\mathrm{T}}\boldsymbol{x}$ weighted with the corresponding spatial frequencies λ_i (normalized with the signal energy $\|\boldsymbol{x}\|^2$), thus resulting in a measure of variation (the larger the smoothness, the larger the level of variation for the graph signal). The range of the smoothness is limited by the maximum Laplacian eigenvalue[2] [34], i.e. $s_{\mathcal{G}}(\boldsymbol{x})\in[0,\max_i\lambda_i]$.

III. GSP-based SHM

We consider a scenario involving a bridge equipped with N sensors, each collecting M temporal measurements each time an event (e.g. a train or vehicle crossing the bridge) is completed, as illustrated in Fig. 1. The eth event is associated to a multivariate time series arranged in a data matrix $\boldsymbol{X}[e]\in\mathbb{R}^{N\times M}$, where $X_{n,m}[e]$ denotes the mth measurement from the nth sensor.

Information about the bridge and sensors placement is assumed to be known in the form of a given adjacency matrix ($\boldsymbol{A}$) representing the topology of the sensor network at each discrete time. The data matrix is split into C non-overlapping snapshots, each collecting data from all the sensors and K consecutive discrete times[3], i.e. the ℓth snapshot from the eth event includes data $\{X_{n,m}[e]\}_{n=1;\ m=(\ell-1)K+1}^{N;\ \ell K}$ arranged in K graph signals $\{\boldsymbol{x}^{(e;\ell)}[k]\}_{k=1}^{K}$ with $x_n^{(e;\ell)}[k]=X_{n,(\ell-1)K+k}[e]$.

A. Spatio-Temporal Graphs

Including the temporal dynamics into the graph representation is crucial to operate with time-series data from sensors. Referring to the generic snapshot from the generic event and omitting here the superscript $(e;\ell)$ for ease of notation, $\boldsymbol{x}[k]$ denotes the graph signal from the kth discrete-time instant, with $k=1,2,\dots,K$.

One possible approach is to extend the concept of graph and corresponding graph signal to a spatio-temporal domain, where each node refers to a specific sensor in a given time instant, and edge representing either spatial or temporal connections among nodes. The spatio-temporal graph is described via the set of nodes and edges and the adjacency matrix. The

[2]The smoothness can also be defined using the normalized graph Lapacian ($\boldsymbol{L}=\boldsymbol{I}-\boldsymbol{D}^{-1/2}\boldsymbol{A}\boldsymbol{D}^{-1/2}$), in which case the upper range limit is 2.

[3]Without loss of generality, we assume that M/K is an integer number.

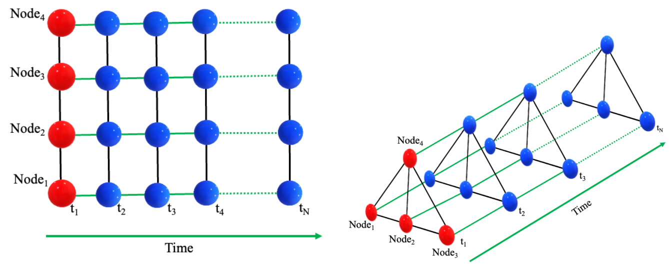

(a) Linear spatial topology (b) Triangular spatial topology

Fig. 2: Spatio-temporal graphs with $N = 4$ sensors and K discrete times. Red nodes denote the spatial placement of the sensors, blue nodes represent their temporal extension. Spatial (resp. temporal) edges are depicted in black (resp. green).

spatio-temporal graph signal ($\tilde{\boldsymbol{x}}$) is defined as the vector stacking the graph signal from each discrete time, i.e. $\tilde{\boldsymbol{x}}^{\mathrm{T}} = \left[\boldsymbol{x}[1]^{\mathrm{T}}, \ldots, \boldsymbol{x}[K]^{\mathrm{T}}\right]$. A similar analysis about the GFT and normalized smoothness can be done by obtaining the corresponding Laplacian matrix (namely spatio-temporal Laplacian matrix ($\tilde{\boldsymbol{L}}$)), related eigendecomposition, and corresponding spatio-temporal normalized smoothness (STNS)

$$\tilde{s}(\tilde{\boldsymbol{x}}) = \frac{\tilde{\boldsymbol{x}}^{\mathrm{T}} \tilde{\boldsymbol{L}} \tilde{\boldsymbol{x}}}{\|\tilde{\boldsymbol{x}}\|^2} \,. \tag{3}$$

where the subscript $\mathcal{G}$ is removed for ease of notation.

In this work, we assume that the topology of the sensor network is invariant with time, thus from a spatial perspective the graph Laplacian matrix ($\boldsymbol{L}$) is a proper representation of the system. Also, from a temporal perspective, we assume that each node is simply connected with its own one-step backward and forward replicas, i.e. the temporal structure is described by the matrix $\boldsymbol{\Theta} \in \mathbb{R}^{K \times K}$ such that

$$\Theta_{i,j} = \begin{cases} 1 & j = i \pm 1 \\ 0 & \text{else} \end{cases} \,.$$

Fig. 2 shows two examples of spatio-temporal graphs with $N = 4$ sensors expanded along K discrete times: the former with a linear spatial topology, the latter with a triangular one. Similar to Eq. (1), a Laplacian matrix for the temporal structure is obtained as

$$\boldsymbol{\Lambda} = \boldsymbol{\Delta} - \boldsymbol{\Theta} \,, \tag{4}$$

where the degree matrix $\boldsymbol{\Delta}$ is a diagonal matrix whose entries on the main diagonal are $\Delta_{i,i} = \sum_{j=1}^{K} \Theta_{i,j}$. Exploring connections beyond a single time step, although potentially beneficial, lies outside the scope of this study.

In case of time-invariant graphs, the spatio-temporal Laplacian matrix can be shown to be expressed as the Cartesian product of the 2 Laplacian matrices [35], i.e.

$$\tilde{\boldsymbol{L}} = \boldsymbol{\Lambda} \times \boldsymbol{L} \,, \tag{5}$$

with $\tilde{\boldsymbol{L}} \in \mathbb{R}^{KN \times KN}$. Also, we have $\tilde{\boldsymbol{x}} \in \mathbb{R}^{KN \times 1}$.

B. Event Anomaly Detection

The proposed SHM system is meant to operate on group of consecutive events, since relying on a single event for damage detection might be unreliable. It is built on the following main steps: (i) compute the STNS statistics of the group of events; (ii) compute the deviation of the group of events from normal operation mode (represented by a reference model) via the KL divergence; (iii) remove the outliers of the sequence of KL-divergence values; and (iv) process the sequence of KL-divergence values after outliers removal with a sequential detection algorithm.

The eth event is associated with a STNS vector $\tilde{\boldsymbol{s}}[e] \in \mathbb{R}^{C \times 1}$, where each entry $\tilde{s}_\ell[e]$ represents a STNS value computed by applying Eq. (3) to the graph signals from the ℓth snapshot. We use the SNTS vector to infer the statistical behaviour of the system and assess if it resembles healthy behavior or significantly deviates from it. We assume that the STNS values follows a Gaussian distribution, given the specific event, and we use the sample mean and sample variance (i.e. the maximum-likelihood estimators [36]) as statistical representation

$$\mu[e] = \frac{1}{C} \sum_{\ell=1}^{C} \tilde{s}_\ell[e] \ , \ \sigma^2[e] = \frac{1}{C} \sum_{\ell=1}^{C} (\tilde{s}_\ell[e] - \mu[e])^2 \,. \tag{6}$$

The KL divergence [37] is a statistical distance commonly used to assess the difference between 2 probability density functions (PDFs). It is worth mentioning that the KL divergence is asymmetric and may be interpreted as a measure of dissimilarity of an arbitrary PDF from a reference PDF. In the specific case that both PDFs are Gaussian, the KL divergence associated to the eth event is expressed as

$$D[e] = \log\left(\frac{\sigma[e]}{\sigma_{\mathrm{H}}}\right) + \frac{(\sigma_{\mathrm{H}}^2 - \sigma^2[e]) - (\mu_{\mathrm{H}} - \mu[e])^2}{2\sigma^2[e]} \,, \tag{7}$$

where μ_{H} and σ_{H}^2 denote the mean and variance, respectively, of the reference Gaussian PFD characterizing the bridge under healthy condition. The reference mean and variance are computed applying Eq. (6) to a vector collecting STNS values from multiple events associated to healthy condition.

As for outliers removal, we apply Tukey's method [38], which operates based on the interquartile range (i.e. the interval encapsulating the central 50% of the data). Any data point outside the interval $[Q_1 - I(Q_3 - Q_1), Q_3 + I(Q_3 - Q_1)]$ is considered an outlier, where Q_1 (resp. Q_3) represents the first (resp. third) quartile of the dataset and I is a parameter usually chosen in the range $[1.5, 3]$.

A sequential detection algorithm, namely EWMA, is then applied to the sequence of KL-divergence values

$$Z_e = \alpha D[e] + (1 - \alpha) Z_{e-1} \,, \tag{8}$$

where Z_e is the decision variable to be compared with a threshold for final decision, and $\alpha \in (0, 1]$ is a parameter trading relevance between current and previous events.

The pseudo-code of the procedure for damage detection is illustrated in Algorithm 1.

Algorithm 1 Damage Detection

Require: $events$, $\boldsymbol{L}$, $\boldsymbol{\Lambda}$, K
$\tilde{\boldsymbol{L}} = \boldsymbol{\Lambda} \times \boldsymbol{L}$
for e in $events$ **do**
  Initialize vector $\tilde{\boldsymbol{s}}[e]$
  for ℓ in e **do**
    $\tilde{\boldsymbol{x}}$ =vectored($\{X_{n,m}[e]\}_{n=1;\ m=(\ell-1)K+1}^{N;\ \ell K}$)
    $\tilde{s}_\ell[e] = \frac{\tilde{\boldsymbol{x}}^{\mathrm{T}}\tilde{\boldsymbol{L}}\tilde{\boldsymbol{x}}}{\|\tilde{\boldsymbol{x}}\|^2}$ ▷ By equation (3)
    $\tilde{\boldsymbol{s}}[e] = \tilde{s}_\ell[e]$
  end for
  $\tilde{\boldsymbol{s}}_{events} = \textsc{Append}(\tilde{\boldsymbol{s}}[e])$
end for
$\mu_{\mathrm{H}}, \sigma^2_{\mathrm{H}} = \textsc{Baseline}(\tilde{\boldsymbol{s}}_{events})$
for e in $events_{New}$ **do**
  Initialize vector $\tilde{\boldsymbol{s}}[e]$
  for ℓ in e **do**
    $\tilde{\boldsymbol{x}}$ =vectored($\{X_{n,m}[e]\}_{n=1;\ m=(\ell-1)K+1}^{N;\ \ell K}$)
    $\tilde{s}_\ell[e] = \frac{\tilde{\boldsymbol{x}}^{\mathrm{T}}\tilde{\boldsymbol{L}}\tilde{\boldsymbol{x}}}{\|\tilde{\boldsymbol{x}}\|^2}$
    $\tilde{\boldsymbol{s}}[e] = \tilde{s}_\ell[e]$
  end for
  $\mu[e], \sigma^2[e] = \textsc{Stats}(\tilde{\boldsymbol{s}}[e])$ ▷ By equation (6)
  $D[e] = \mathrm{KL}(\mu[e], \sigma^2[e], \mu_{\mathrm{H}}, \sigma^2_{\mathrm{H}})$ ▷ By equation (7)
end for
$\boldsymbol{D}_{filtered} = \textsc{OutlierRemoval}(\boldsymbol{D})$
$\boldsymbol{Z} = \mathrm{EWMA}(\boldsymbol{D}_{filtered})$ ▷ By equation (8)
UCL, LCL $= \mathrm{CL}(\mu_{\mathrm{H}}, \sigma^2_{\mathrm{H}})$ ▷ By equation (9) and (10)
if LCL $\leq \boldsymbol{Z} \leq$ UCL **then**
  Decision: Healthy
else
  Decision: Damage
end if

IV. Data Description

The two datasets used for validating our work are described here: one is generated via numerical simulations (namely *Case Study 1*) and one is obtained from real-world measurements (namely *Case Study 2*). The two datasets are not related each other and are treated separately to demonstrate the effectiveness of the proposed algorithm on both synthetic and real-world scenarios. The minimum number of sensors and related positions were strategically selected to capture the first three modes of the bridge. In scenarios with a many sensors, these were placed at regular (spatial) intervals.

A. Case Study 1: Dataset from Numerical Simulations

The considered numerical model integrates the behaviors of the train, the ballasted track, and the bridge:

- The train is modeled as a sequence of consecutive vehicles, each characterized by a multi-body system with six degrees of freedom. This model includes a primary suspension system that connects the two axles of each bogie and a secondary suspension system that supports the main body [39].
- The track is modeled identifying rails, pad, sleeper, ballast, and sub-ballast. More specifically, we employed Class-6 track irregularities from the Federal Railroad Administration [40]. The rail is modeled as a beam, while the other components are treated as lumped masses.
- The bridge is modeled using a Finite Element Model (FEM) based on Euler-Bernoulli beam theory. Each element comprises 2 nodes with two degrees of freedom per node (specifications in Table I).

TABLE I: Bridge specifications.

Bridge Specifications	Value
Length (m)	50
Second Moment of Area (m^4)	51.3
Mass per Unit Length (kg/m)	69000
Modulus of Elasticity ($\mathrm{N/m}^2$)	3.5×10^{10}

TABLE II: Variability of the train-model parameters.

	Min.	Max.	Mean	St. Dev.
Velocity (km/h)	150	170	160	3
Body Mass (kg)	42100	53500	47800	500

Our study examines an ICE3 Velaro train configuration comprised of 8 wagons, with mechanical properties and dimensions as in [41]. To ascertain dynamic stability before the train's entry onto the bridge, we model a $100\ \mathrm{m}$ extension beyond the bridge using a standard UIC60 rail design and a sleeper spacing of $0.6\ \mathrm{m}$. The presented train-track-bridge simulation tool is available in [39] together with additional descriptions.

In this work, we assume that the train speed and body mass vary for each event (according to Table II), while the train's suspension properties remain constant. In addition, 3 different damage cases (DCs) are considered to demonstrate the effectiveness of the proposed SHM approach, each with a different location of the damage:

- **DC1** - damage location is at the midpoint of the the first half of the bridge;
- **DC2** - damage location is at the midpoint of the bridge;
- **DC3** - damage location is at the midpoint of the the second half of the bridge.

The damage was modelled using 20% stiffness loss at each location. For each case, 300 events were generated: 200 in healthy scenario and 100 in presence of damages. Each event contains the values of the accelerations from the bridge with white noise added to mimic measurement noise[4].

B. Case Study 2: Data from Real-World Measurements

We considered signals from a bridge in Leuven, Belgium, known as the KW51 railway bridge [42]. Spanning $115\ \mathrm{m}$ in length and $12.4\ \mathrm{m}$ in width, this bridge features 2 separated ballasted tracks situated at the north and south sides (namely Track A and Track B). Both tracks have a curved horizontal alignment, with an enforced speed limit of $160\ \mathrm{km/h}$ for passenger trains. The bridge's monitoring system provides data in 3 different periods (starting from September 2018) experiencing different bridge conditions: (i) the first period

[4]A truncated Gaussian noise is selected to reproduce signal-to-noise ratios within the range [25dB, 35dB], see also [23]

TABLE III: Sensors' relative position along the bridge.

N	Relative Positions
3	3/50, 1/2, 47/50
5	3/50, 6/25, 1/2, 19/25, 47/50
9	3/50, 7/50, 6/25, 9/25, 12/25, 29/50, 7/10, 8/10, 47/50

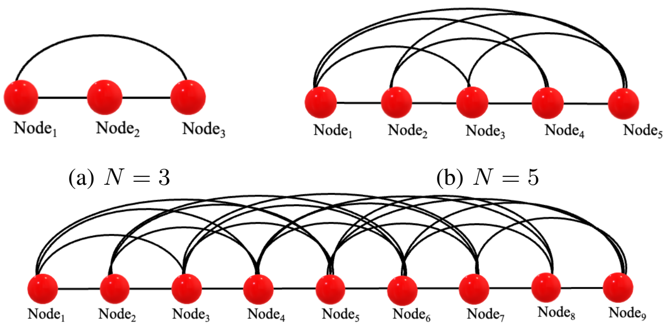

(a) $N = 3$ (b) $N = 5$

(c) $N = 9$

Fig. 3: Spatial topology.

consists of 7.5-month measurements under normal conditions; (ii) the second period includes 4.5 months of measurements from the retrofit installation, namely **RI** case; and (iii) the final period features 3.5 months of measurements from the strengthened bridge, namely **SB** case.

V. Results and Discussion

Data have been processed using MATLAB according to the algorithm described in Sec. III.

A. Case Study 1: Results on Simulated Data

Scenarios with $N \in \{3, 5, 9\}$ aligned sensors are considered, with Tab. III providing the relative location of the sensors along the bridge (0 and 1 represents the two ends of the bridge). As for the spatial topology, fully-connected topology is assumed in both cases $N = 3$ and $N = 5$, while in the case $N = 9$ two sensors are connected if at most 3 sensors are found in between them. Fig. 3 shows the spatial topology of the three considered scenarios. A fully-connected topology allows to infer the dependencies among sensor measurements in the most comprehensive way, but it is also the most expensive topology in terms of computational complexity. For small-size systems ($N = 3$ and $N = 5$) the complexity is not prohibitive even in the case of fully-connected topology. Differently, for the case with $N = 9$, we considered reduced number of connections for complexity issues. The impact of the number of connections on the inference capability falls beyond the scope of this paper. As for the temporal extension, $K = 512$ discrete-time instants are considered, with $M = 7800$ samples per event generated[5].

In order to provide a visual representation of the impact on the smoothness of healthy and damaged bridge conditions, we compute (per event) the following statistics of the smoothness: max, min, mean, and standard deviation. Fig. 4 shows the smoothness statistics for the scenario with $N = 5$ sensors considering the 3 damaged cases (DC1, DC2, and DC3) compared with the normal condition (Healthy). Other scenarios are not shown here for brevity. Apparently, the smoothness behavior is affected by the absence/presence of structural damages, but unfortunately no specific statistic (or combination of statistics) showed to work effectively in all considered cases[6]. This motivated the use of a more general metric like the KL divergence for the final detection.

Figs. 5, 6 and 7 depict the damage index (Z) for various scenarios and damage cases[7]. More specifically, the first 60 events represent healthy data and are used to establish the baseline distribution. The remaining part is made of 140 healthy events and 100 damaged events, showing the effectiveness of the proposed methodology. It is apparent how the damage index behavior is significantly affected by the presence of a damage and how different locations of the damage have different impact. More specifically, Figs. 5, 6 and 7 show that the change in the damage index (Z) is more pronounced in DC2 than DC1 and DC3 for all three sensor configurations, suggesting that the damage index might include information related to damage localization and damage-magnitude estimation. However, given our focus on damage detection, those tasks are beyond the scope of this paper.

A detection system should finally take decisions based on a threshold-based rule, however hyper-parameter optimization and assessment of detection performance fall beyond the scope of the paper. To provide an insight on the potential value of the proposed methodology, Figs. 5, 6 and 7 show possible upper and lower control limits (UCL and LCL), computed as [43]

$$\mathrm{UCL}_e = \mu_{\mathrm{H}} + 7\sigma_{\mathrm{H}} \sqrt{\frac{\alpha}{(2-\alpha)} \left[1 - (1-\alpha)^{2e}\right]}\,, \tag{9}$$

$$\mathrm{LCL}_e = \mu_{\mathrm{H}} - 7\sigma_{\mathrm{H}} \sqrt{\frac{\alpha}{(2-\alpha)} \left[1 - (1-\alpha)^{2e}\right]}\,. \tag{10}$$

In all cases, damage-index values fall inside (resp. outside) the considered bounds when the damage is absent (resp. present), thus confirming the validity of the proposed approach.

Also, Fig. 8 shows the ROC curves for each damage case to further illustrate the implications of threshold selection in terms of probability of detection and probability of false alarm. It can be noticed how misclassifications are reduced when increasing the number of sensors with the $N = 3$ scenario showing worse (but still sufficiently good) performance. The gap between scenarios with increasing number of sensors (N) seems to saturate to attractive performance levels, thus suggesting that the proposed approach does not require large number of sensors.

B. Case Study 2: Results on Real-World Measurements

We construct a graph using four sensors arranged in a triangular spatial topology as in Fig. 2b. These sensors are part of the original six that were installed on the bridge, each measuring acceleration in the horizontal and vertical directions

[5]The last 120 samples are discarded.

[6]In the specific case shown here, the maximum value of the smoothness is the most effective indicator.

[7]Tukey's method is implemented using non-overlapping windows with size 20 and tuned with $I = 3$, while EWMA is tuned with $\alpha = 0.05$.

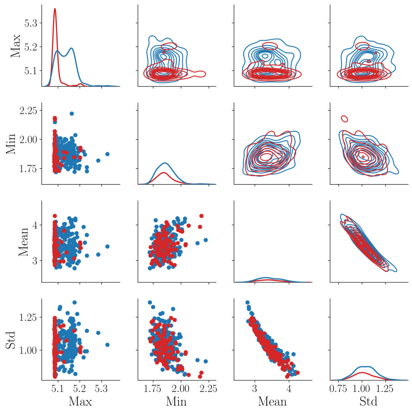

(a) DC1

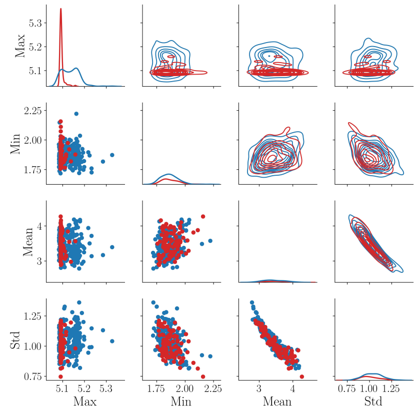

(b) DC2

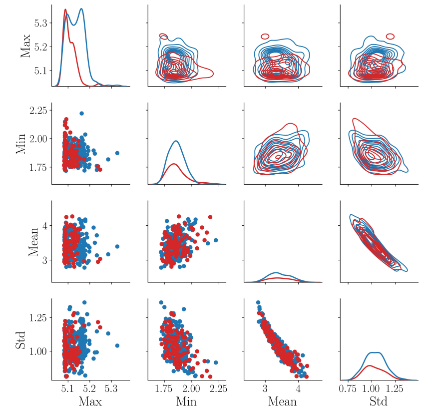

(c) DC3

Fig. 4: Smoothness statistics with $N = 5$ sensors. Simulated data. Healthy (resp. damaged) conditions in blue (resp. red).

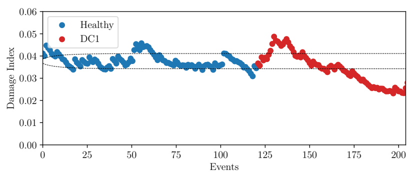

(a) DC1

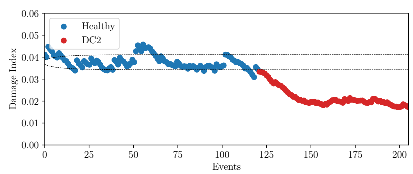

(b) DC2

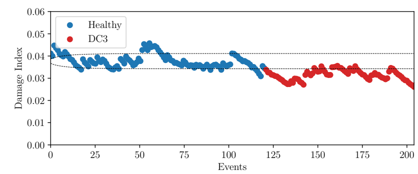

(c) DC3

Fig. 5: Damage index with $N = 3$ sensors. Simulated data.

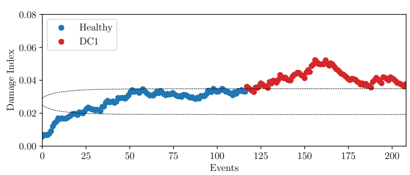

(a) DC1

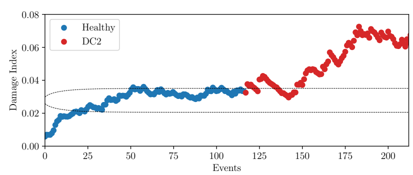

(b) DC2

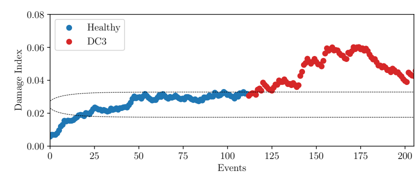

(c) DC3

Fig. 6: Damage index with $N = 5$ sensors. Simulated data.

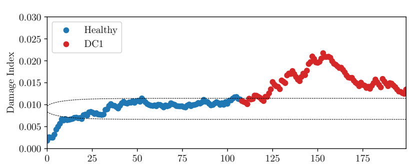

(a) DC1

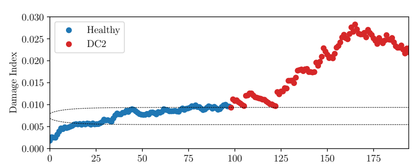

(b) DC2

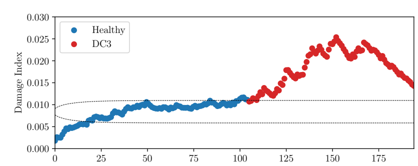

(c) DC3

Fig. 7: Damage index with $N = 9$ sensors. Simulated data.

[42]: those measuring the acceleration in the vertical direction are selected in this work. As for the temporal extension, $K = 16$ discrete-time instants are considered.

Fig. 9 shows the smoothness statistics for the scenario with $N = 4$ sensors considering the 2 damaged cases (RI and SB) compared with the normal condition (Healthy). It is interesting to notice that the RI case exhibits different statistics than the Healthy case, while the difference is largely reduced when comparing the SB and Healthy cases, i.e. the strengthening intervention somehow makes the bridge to behave similarly to the normal condition.

Fig. 10 depicts the damage index (Z) for the considered case with real-world measurement[8]. More specifically, the first 60 events represent healthy data and are used to establish the baseline distribution. The remaining part is made of 222 healthy events, 149 events with RI case and 129 events with SB case. It is apparent how the results from the real-world measurements confirm that the proposed damage index is a relevant candidate for the design of effective SHM systems. Additionally, the interesting behavior of the RI and SB cases with respect to the Healthy case, suggests that the proposed damage index might be also useful to quickly assess the

[8]Similar setting as with simulated data is assumed for Tukey's method and EWMA. UCL and LCL curves are also shown.

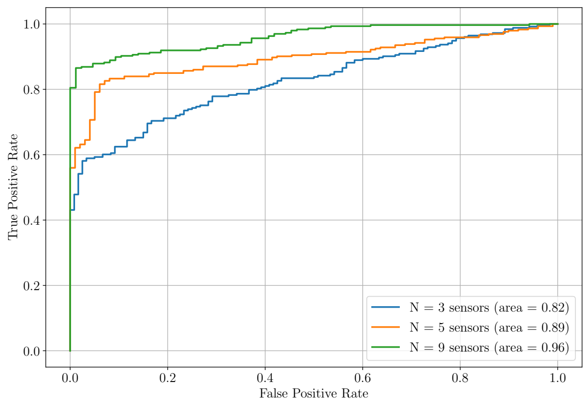

Fig. 8: ROC curves for the numerical data.

validation of maintenance/repairing operations.

Also, Fig. 11 shows the ROC curve for the damage detection in real-world data, again showing the implications of threshold selection in terms of probability of detection and probability of false alarm.

As for performance comparison in the case of real-world measurements, we also implemented a monitoring procedure based on Operational Modal Analysis (OMA) on an hourly basis, utilizing ambient vibration data from the KW 51 Bridge. OMA is a popular method to identify modal frequencies and mode shapes of bridges, often employed for damage evaluation. More specifically, the modal frequencies were derived according to [44] and signals analyzed via the covariance-driven stochastic subspace identification algorithm [45] and clustering approach recommended in [46]. To provide a fair comparison with the proposed method, only global vertical modes were considered. Furthermore, an unsupervised deep learning method based on a Probabilistic Temporal Autoencoder (PTAE) [47] has been considered as performance bound.

Table IV presents the performance comparison regarding accuracy, precision, and recall, where the Upper Control Limit UCL and LCL were utilized as detection thresholds for the proposed GSP-based approach and both the OME and the PTAE benchmarks. In the case of OMA, a one-class Support Vector Machine (SVM) [48] was employed for damage detection. It is worth mentioning that no optimization analysis was performed for both approaches, so no optimality claim in terms of performance. Also, OMA can be considered a traditional approach while PTAE can be considered a recent AI-based approach. Our proposed method slightly outperforms the former, while exhibits some performance gap with the latter. On a different note, we believe it important to stress that similar performance to traditional approaches were achieved with the proposed GSP-based methods despite requiring lower computational cost and having no critical dependency on some crucial parameter. From a computational perspective, the OMA-based approach require singular value decomposition of covariance matrices and is quite sensitive to system-order selection. On the other hand, deep learning methods require a substantial amount of data and significant computational resources to train and run the model. It involves learning thousands of parameters and their utilization in bridge assessments, making it resource-intensive and potentially inefficient for resource and energy-constrained devices. In addition, deel-learning models might be problematic to adopt in safety-critical systems due to their black-box inherent behaviour and poor *explanaibility*. Conversely, the proposed GSP-based approach appears a very promising candidate from performance, computational-complexity, robustness and explainability points of view.

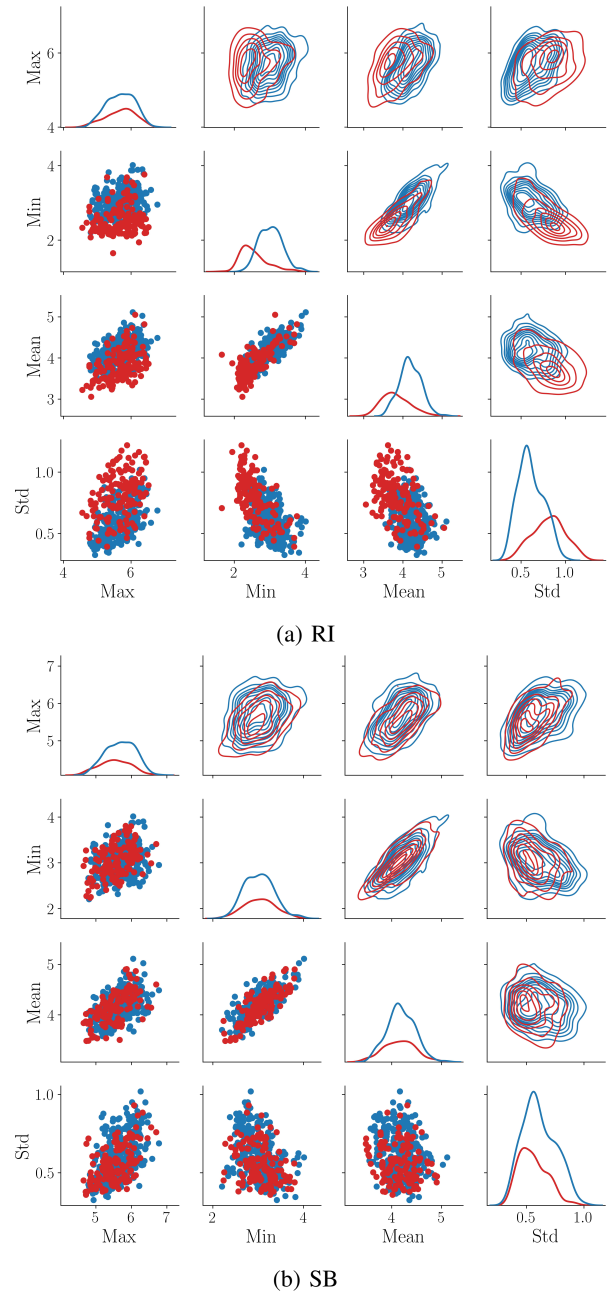

Fig. 9: Smoothness statistics with $N = 4$ sensors. Real-world measurements. Healthy (resp. damaged) conditions in blue (resp. red).

VI. Conclusion and Future Work

We proposed a GSP-based algorithm for SHM of bridges which effectively exploits both spatial and temporal structure

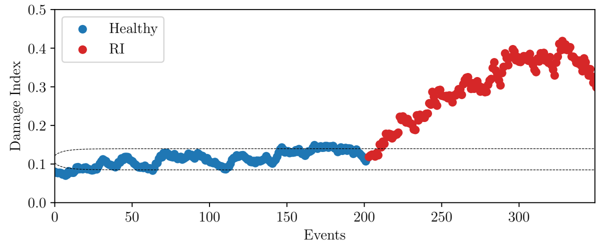

(a) RI

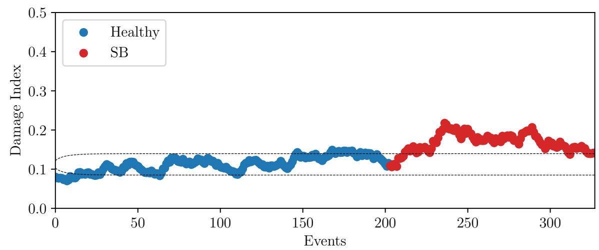

(b) SB

Fig. 10: Damage index with $N = 4$ sensors. Real-world measurements.

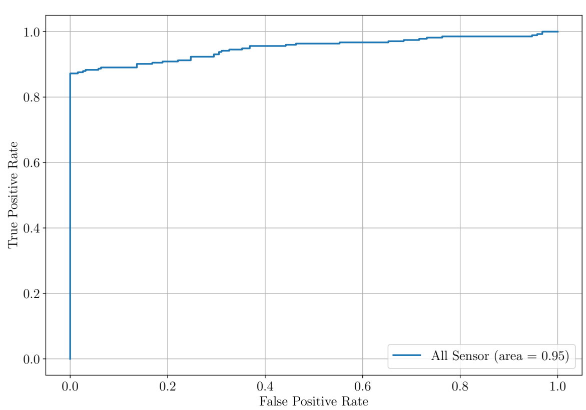

Fig. 11: ROC curve for the experimental data.

TABLE IV: Performance comparison using real-world measurements.

	RI case			SB case		
	GSP	OMA	PTAE	GSP	OMA	PTAE
Accuracy	93.4%	87.5%	97.6%	89.6%	96.5%	95.3%
Precision	89.2%	92%	96.7%	87.3%	86.8%	96.1%
Recall	95.0%	76.2%	99.3%	87.3%	100%	95.3%

of data collected from sensors. Spatio-temporal graphs seemed the natural formal structure for representing the sensors data and related bridge behaviour. The proposed algorithm processes sensor data via low-complexity GSP techniques, then KL divergence, Tukey's outlier method and EWMA filtering are combined for damage detection. The assumption that structural damages impact the statistics of the smoothness of the corresponding graphs has been validated analyzing data collected both from numerical simulations and from real-world measurements. Comparisons with standard solutions from common practice in structural engineering seem very promising and make GSP-based solutions potentially suitable for cost-effective and resource-efficient real-time SHM systems. Future work should focus on performing damage localization using the proposed GSP-based methodology.

REFERENCES

[1] S. Bloemheuvel, J. van den Hoogen, and M. Atzmueller, "Graph signal processing on complex networks for structural health monitoring," in *International Conference on Complex Networks and Their Applications (Springer)*, 2021, pp. 249–261.

[2] A. Ortega, P. Frossard, J. Kovačević, J. M. Moura, and P. Vandergheynst, "Graph signal processing: Overview, challenges, and applications," *Proceedings of the IEEE*, vol. 106, no. 5, pp. 808–828, Apr. 2018.

[3] H. Darvishi, D. Ciuonzo, and P. Salvo Rossi, "Deep recurrent graph convolutional architecture for sensor fault detection, isolation, and accommodation in digital twins," *IEEE Sensors Journal*, vol. 23, no. 23, pp. 29 877–29 891, 2023.

[4] Z. Xing, S. Zhao, W. Guo, F. Meng, X. Guo, S. Wang, and H. He, "Coal resources under carbon peak: Segmentation of massive laser point clouds for coal mining in underground dusty environments using integrated graph deep learning model," *Energy*, vol. 285, p. 128771, 2023.

[5] B. F. Spencer Jr, V. Hoskere, and Y. Narazaki, "Advances in computer vision-based civil infrastructure inspection and monitoring," *Engineering*, vol. 5, no. 2, pp. 199–222, Apr. 2019.

[6] H. Nick and A. Aziminejad, "Vibration-based damage identification in steel girder bridges using artificial neural network under noisy conditions," *Journal of Nondestructive Evaluation*, vol. 40, pp. 1–22, Jan. 2021.

[7] Z. Lingxin, S. Junkai, and Z. Baijie, "A review of the research and application of deep learning-based computer vision in structural damage detection," *Earthquake Engineering and Engineering Vibration*, vol. 21, no. 1, pp. 1–21, Jan. 2022.

[8] Y. An, E. Chatzi, S.-H. Sim, S. Laflamme, B. Blachowski, and J. Ou, "Recent progress and future trends on damage identification methods for bridge structures," *Structural Control and Health Monitoring*, vol. 26, no. 10, p. e2416, Jul. 2019.

[9] Y. Zhang and K.-V. Yuen, "Review of artificial intelligence-based bridge damage detection," *Advances in Mechanical Engineering*, vol. 14, no. 9, Sep. 2022.

[10] A. Moallemi, A. Burrello, D. Brunelli, and L. Benini, "Exploring scalable, distributed real-time anomaly detection for bridge health monitoring," *IEEE Internet of Things Journal*, vol. 9, no. 18, pp. 17 660–17 674, 2022.

[11] O. Avci, O. Abdeljaber, S. Kiranyaz, M. Hussein, M. Gabbouj, and D. J. Inman, "A review of vibration-based damage detection in civil structures: From traditional methods to machine learning and deep learning applications," *Mechanical Systems and Signal Processing*, vol. 147, Jan. 2021.

[12] M. M. Alamdari, K. Kildashti, B. Samali, and H. V. Goudarzi, "Damage diagnosis in bridge structures using rotation influence line: Validation on a cable-stayed bridge," *Engineering Structures*, vol. 185, pp. 1–14, Apr. 2019.

[13] F. Huseynov, C. Kim, E. J. Obrien, J. Brownjohn, D. Hester, and K. Chang, "Bridge damage detection using rotation measurements–experimental validation," *Mechanical Systems and Signal Processing*, vol. 135, Jan. 2020.

[14] E. J. Obrien, J. Brownjohn, D. Hester, F. Huseynov, and M. Casero, "Identifying damage on a bridge using rotation-based bridge weigh-in-motion," *Journal of Civil Structural Health Monitoring*, vol. 11, pp. 175–188, Oct. 2021.

[15] S. Quqa, L. Landi, and P. P. Diotallevi, "Automatic identification of dense damage-sensitive features in civil infrastructure using sparse sensor networks," *Automation in Construction*, vol. 128, Aug. 2021.

[16] ——, "Instantaneous identification of densely instrumented structures using line topology sensor networks," *Structural Control and Health Monitoring*, vol. 29, no. 3, Nov. 2022.

[17] B. Bhowmik, T. Tripura, B. Hazra, and V. Pakrashi, "First-order eigen-perturbation techniques for real-time damage detection of vibrating systems: Theory and applications," *Applied Mechanics Reviews*, vol. 71, no. 6, p. 060801, 2019.

[18] ——, "Real time structural modal identification using recursive canonical correlation analysis and application towards online structural damage detection," *Journal of Sound and Vibration*.

[19] Z. Deng, M. Huang, N. Wan, and J. Zhang, "The current development of structural health monitoring for bridges: A review," *Buildings*, vol. 13, no. 6, p. 1360, 2023.
[20] M. Tang, J. Cao, and X. Jia, "Efficient power management for wireless sensor networks: A data-driven approach," in *2008 33rd IEEE Conference on Local Computer Networks (LCN)*. IEEE, 2008, pp. 106–113.
[21] H. Fu, Z. S. Khodaei, and M. F. Aliabadi, "An event-triggered energy-efficient wireless structural health monitoring system for impact detection in composite airframes," *IEEE Internet of Things Journal*, vol. 6, no. 1, pp. 1183–1192, 2018.
[22] M. Z. Sarwar, M. R. Saleem, J.-W. Park, D.-S. Moon, and D. J. Kim, "Multimetric event-driven system for long-term wireless sensor operation for shm applications," *IEEE Sensors Journal*, vol. 20, no. 10, pp. 5350–5359, 2020.
[23] M. Z. Sarwar and D. Cantero, "Vehicle assisted bridge damage assessment using probabilistic deep learning," *Measurement*, vol. 206, Jan. 2023.
[24] Y.-W. Wang, Y.-Q. Ni, and S.-M. Wang, "Structural health monitoring of railway bridges using innovative sensing technologies and machine learning algorithms: a concise review," *Intelligent Transportation Infrastructure*, vol. 1, Sep. 2022.
[25] I. Gonzalez and R. Karoumi, "BWIM aided damage detection in bridges using machine learning," *Journal of Civil Structural Health Monitoring*, vol. 5, pp. 715–725, Aug. 2015.
[26] A. C. Neves, I. González, and R. Karoumi, "Development and validation of a data based SHM method for railway bridges," *Structural Health Monitoring Based on Data Science Techniques*, pp. 95–116, Oct. 2022.
[27] L. Li, G. Liu, L. Zhang, and Q. Li, "Fs-lstm-based sensor fault and structural damage isolation in shm," *IEEE Sensors Journal*, vol. 21, no. 3, pp. 3250–3259, 2020.
[28] M. R. Azim and M. Gül, "Damage detection of steel girder railway bridges utilizing operational vibration response," *Structural Control and Health Monitoring*, vol. 26, no. 11, Aug. 2019.
[29] A. Meixedo, J. Santos, D. Ribeiro, R. Calçada, and M. Todd, "Damage detection in railway bridges using traffic-induced dynamic responses," *Engineering Structures*, vol. 238, Jul. 2021.
[30] M. Lydon, S. E. Taylor, D. Robinson, P. Callender, C. Doherty, S. K. Grattan, and E. J. O'Brien, "Development of a bridge weigh-in-motion sensor: performance comparison using fiber optic and electric resistance strain sensor systems," *IEEE Sensors Journal*, vol. 14, no. 12, pp. 4284–4296, 2014.
[31] A. Sabato, S. Dabetwar, N. N. Kulkarni, and G. Fortino, "Non-contact sensing techniques for ai-aided structural health monitoring: a systematic review," *IEEE Sensors Journal*, 2023.
[32] A. Sandryhaila and J. M. Moura, "Discrete signal processing on graphs: Graph fourier transform," in *IEEE International Conference on Acoustics, Speech and Signal Processing*, 2013, pp. 6167–6170.
[33] E. Isufi, A. S. Mahabir, and G. Leus, "Blind graph topology change detection," *IEEE Signal Processing Letters*, vol. 25, no. 5, pp. 655–659, Mar. 2018.
[34] C. Hu, J. Sepulcre, K. A. Johnson, G. E. Fakhri, Y. M. Lu, and Q. Li, "Matched signal detection on graphs: Theory and application to brain imaging data classification," *NeuroImage*, vol. 125, pp. 587–600, Jan. 2016.
[35] F. Grassi, A. Loukas, N. Perraudin, and B. Ricaud, "A time-vertex signal processing framework: Scalable processing and meaningful representations for time-series on graphs," *IEEE Transactions on Signal Processing*, vol. 66, no. 3, pp. 817–829, Nov. 2017.
[36] S. M. Kay, *Fundamentals of statistical signal processing: estimation theory*. Prentice-Hall, Inc., 1993.
[37] T. M. Cover, *Elements of information theory*. John Wiley & Sons, 1999.
[38] J. W. Tukey *et al.*, *Exploratory data analysis*. Reading, MA, 1977, vol. 2.
[39] D. Cantero, "TTB-2D: Train–Track–Bridge interaction simulation tool for Matlab," *SoftwareX*, vol. 20, pp. 1–6, Oct. 2022.
[40] L. Fryba and W. Courage, "Dynamics of railway bridges," *Meccanica*, vol. 32, no. 1, pp. 95–95, 1997.
[41] K. N. Gia, J. M. G. Ruigómez, and F. G. Castillo, "Influence of rail track properties on vehicle–track responses," vol. 168, no. 6, pp. 499–509, Dec. 2015.
[42] K. Maes, L. Van Meerbeeck, E. Reynders, and G. Lombaert, "Validation of vibration-based structural health monitoring on retrofitted railway bridge KW51," *Mechanical Systems and Signal Processing*, vol. 165, pp. 1–24, Sep. 2021.
[43] D. C. Montgomery, *Introduction to statistical quality control*. John wiley & sons, 2019.
[44] K. Maes and G. Lombaert, "Monitoring railway bridge KW51 before, during, and after retrofitting," *Journal of Bridge Engineering*, vol. 26, no. 3, pp. 1–19, Jan. 2021.
[45] B. Peeters and G. De Roeck, "Reference-based stochastic subspace identification for output-only modal analysis," *Mechanical Systems and Signal Processing*, vol. 13, no. 6, pp. 855–878, Nov. 1999.
[46] F. Magalhães, A. Cunha, and E. Caetano, "Online automatic identification of the modal parameters of a long span arch bridge," *Mechanical Systems and Signal Processing*, vol. 23, no. 2, pp. 316–329, Feb. 2009.
[47] M. Z. Sarwar and D. Cantero, "Probabilistic autoencoder-based bridge damage assessment using train-induced responses," *Mechanical Systems and Signal Processing*, vol. 208, p. 111046, 2024.
[48] S. Yin, X. Zhu, and C. Jing, "Fault detection based on a robust one class support vector machine," *Neurocomputing*, vol. 145, pp. 263–268, Dec. 2014.

Muhammad Asaad Cheema (Member, IEEE) received his Master's degree in Electrical Engineering from the National University of Sciences and Technology (NUST) in Islamabad, Pakistan. During his MS at NUST, he had the opportunity to spend one semester on the ERASMUS+ mobility program at Frederick University, Cyprus, from October 2019 to January 2020. Currently, he is pursuing his PhD at the Norwegian University of Science and Technology, with the SPIN group. His research interests include Graph Signal Processing, Machine Learning, and the Internet of Things (IoT).

Muhammad Zohaib Sarwar obtained his Bachelor's degree in Electronic Engineering from Bahria University, Pakistan, in 2017. He continued his education at Chung-Ang University in Seoul, South Korea, earning a Master's in Structural Engineering in 2019 from the Smart Infrastructure Technology Laboratory (SITL).In 2023, he achieved his Ph.D. in Structural Engineering from the Norwegian University of Science and Technology (NTNU), Norway. Presently, he serves as a Postdoctoral Fellow at NTNU.

His research focuses on structural health monitoring. He has shown interest in wireless smart sensor networks, sensor fusion, and the integration of machine learning techniques, especially physics-guided machine learning, for comprehensive structural assessment.

Vinay Chakravarthi Gogineni (Senior Member, IEEE) received the Bachelor's degree in electronics and communication engineering from Jawaharlal Nehru Technological University, Andhra Pradesh, India, in 2005, the Master's degree in communication engineering from VIT University, India, in 2008, and the Ph.D. degree in electronics and electrical communication engineering from Indian Institute of Technology Kharagpur, India in 2019. Currently, he is an Assistant Professor at SDU Applied AI and Data Science, The Maersk Mc-Kinney Moller Institute, University of Southern Denmark, Denmark. Prior to this he worked as a postdoctoral research fellow at NTNU and Simula, Norway. From 2008 to 2011, he was with a couple of MNCs in India.

His research interests include machine learning, distributed machine learning, geometric deep learning, machine unlearning and their application in healthcare, industrial internet-of-things and fusion energy. He was a recipient of the ERCIM Alain Bensoussan Fellowship in 2019 and the Best Paper Award at APSIPA ASC-2021, Tokyo, Japan. He is a member of the editorial board for the IEEE Sensors Journal.

Daniel Cantero received the integrated degree (Bachelor+Master) in civil engineering from the University of Granada, Spain, in 2005, and a Ph.D. in bridge dynamics from the University College Dublin, Ireland, in 2010. He worked as a postdoctoral researcher in industry and academia at Plaxis BV, The Netherlands; Trinity College Dublin, Ireland; Roughan & O'Donovan, Ireland; KTH Royal Institute of Technology, Sweden; Norwegian University of Science and Technology (NTNU), Norway. Since July 2017, Daniel is an Associate Professor with the Department of Structural Engineering at NTNU.

Pierluigi Salvo Rossi (Senior Member, IEEE) was born in Naples, Italy, in 1977. He received the Dr.Eng. degree (*summa cum laude*) in telecommunications engineering and the Ph.D. degree in computer engineering from the University of Naples "Federico II", Italy, in 2002 and 2005, respectively. He is currently a Full Professor and the Deputy Head with the Department Electronic Systems, Norwegian University of Science and Technology (NTNU), Trondheim, Norway. He is also the Deputy Manager of the Centre for Green Shift in the Built Environment, NTNU, Trondheim, Norway and a part-time Research Scientist with the Department Gas Technology, SINTEF Energy Research, Norway.

Previously, he worked with the University of Naples "Federico II", Italy, with the Second University of Naples, Italy, with NTNU, Norway, and with Kongsberg Digital AS, Norway. He held visiting appointments with Drexel University, USA, Lund University, Sweden, NTNU, Norway, and Uppsala University, Sweden. His research interests fall within the areas of communication theory, data fusion, machine learning, and signal processing.

Prof. Salvo Rossi was awarded as an Exemplary Senior Editor of the IEEE COMMUNICATIONS LETTERS in 2018. He is (or has been) in the Editorial Board of the IEEE SENSORS JOURNAL, the IEEE OPEN JOURNAL OF THE COMMUNICATIONS SOCIETY, the IEEE TRANSACTIONS ON SIGNAL AND INFORMATION PROCESSING OVER NETWORKS, the IEEE COMMUNICATIONS LETTERS, and the IEEE TRANSACTIONS ON WIRELESS COMMUNICATIONS.